Am J Cancer Res 2025;15(12):5266-5280
www.ajcr.us /ISSN:2156-6976/ajcr0169650

Original Article

ZNF710 regulates the proliferation, migration, apoptosis, and cell cycle progression of gastric cancer cells through the Wnt/β-catenin pathway

Runkai Zhou[1*], Jingyi Zhou[2*], Jinfeng Cai[1*], Jiazhe Wen[3], Fazhi Wang[1], Di Ma[2], Qingshan Luo[1], Abudushalamu Yalikun[1], Jinlu Han[4], Xuefeng Zhou[5], Yang Yu[1], Qi Li[2], Yugang Wen[1]

[1]Department of General Surgery, Shanghai General Hospital, Shanghai Jiao Tong University School of Medicine, Shanghai 200080, China; [2]Department of Oncology, Shanghai General Hospital, Shanghai Jiao Tong University School of Medicine, Shanghai 200080, China; [3]School of Basic Medical Sciences, Fudan University, Shanghai 200032, China; [4]Department of Gastroenterology, Shanghai Tong Ren Hospital, Shanghai Jiao Tong University School of Medicine, Shanghai 200336, China; [5]Department of Oncology, The Dongtai Hospital of Nantong University, Yancheng 224200, Jiangsu China. [*]Equal contributors.

Received October 29, 2025; Accepted December 17, 2025; Epub December 25, 2025; Published December 30, 2025

Abstract: Objective: This study aimed to investigate the mechanism underlying the role of Zinc finger protein 710 (ZNF710) in gastric cancer (GC). Methods: The level of ZNF710 expression in GC and its prognosis were examined based on the public databases and clinical samples. Cell models of lentivirus-mediated overexpression (oeZNF710) and knockdown (shZNF710) of ZNF710 were developed on the AGS and HGC-27 GC cell lines. The biological behaviors of these cells were analysed systematically, comprising proliferation (as measured by CCK-8 assay and plate cloning experiment), apoptosis (measured by flow cytometry), and migration (measured by Transwell assay). To confirm the expression of the main proteins of the Wnt/β-catenin system, western blotting analysis was conducted. Besides, functional rescue experiments of Wnt signaling agonist SKL2001 and Wnt signaling inhibitor XAV939 were performed. The in vivo activity of ZNF710 was tested in a nude mouse subcutaneous xenograft model. Results: The expression of ZNF710 was significantly increased in GC tissues and cell lines compared to standard controls, whereas high levels of ZNF710 were associated with a poor prognosis in GC patients. ZNF710 knockdown of HGC-27 cells significantly reduced cell proliferation, migration, and invasion and increased apoptosis. On the contrary, overexpression of ZNF710 in AGS cells produced the reverse effects. Mechanistically, ZNF710 overexpression increased the expression of Wnt/β-catenin pathway-related regulatory proteins, and ZNF710 knockdown reduced their expression. Conclusion: ZNF710 is highly expressed in GC and promotes GC cell proliferation, migration, and invasion while inhibiting apoptosis by activating the Wnt/β-catenin pathway, suggesting it may serve as a potential therapeutic target for GC.

Keywords: Zinc finger protein, gastric cancer, Wnt/β-catenin, cell cycle

Introduction

Gastric cancer (GC) ranks as the fifth most prevalent malignancy globally [1]. High-incidence regions for GC include East Asia and Eastern Europe [2]. Common risk factors for GC mainly include dietary habits, family history, EB virus infection, Helicobacter pylori infection, and smoking [3-5]. Unfortunately, symptoms of GC are not prominent in the early stages, and they are often diagnosed in the advanced stages, resulting in a poor prognosis [6]. Surgical treatment, especially D2 lymph node dissection, is the main treatment method for GC; however, its success rate is limited. The other modalities of treatment have demonstrated limited effect in patients with advanced GC as well [7]. Thus, the discovery of novel specific tumour biomarkers or functional proteins is of great significance in the diagnosis, prevention, and therapy of GC in its early stage.

Zinc finger proteins are key components in the regulation of gene expression and affect many

https://doi.org/10.62347/HCCY8796

critical biological processes within cells [8, 9]. Zinc finger proteins are extensively involved in diverse biological functions within the body, including transcriptional regulation, RNA binding, interactions between proteins, DNA recombination and repair, and cell cycle regulation [10]. Zinc finger protein 710 (ZNF710) is a member of the zinc finger protein family, which plays an important role in tumor activity [11-13]. Previous studies have confirmed the role of ZNF710 in regulating the activity of renal cancer cells [14]. In GC, immune-related lncRNA ZNF710-AS1-201 facilitates the metastasis and invasion of GC cells [15]. Notably, the specific role and underlying molecular mechanism of ZNF710 in GC have not been systematically investigated.

Zinc finger proteins are closely related to some canonical signaling pathways, typically regulating downstream pathways through molecular interactions to alter the biological characteristics of tumor cells. The Wnt signaling pathway is one such example [16]. The classical Wnt pathway, Wnt/β-catenin, is closely related to the progression of a variety of tumors [17]. For GC, Wnt/β-catenin has been confirmed to be involved in the process of autophagy, ferroptosis and many other life activities of GC cells [18, 19]. Moreover, Wang Y et al. also found that Wnt/β-catenin was related to chemotherapy resistance of GC [20].

In this study, we innovatively propose that ZNF710 regulates multiple biological characteristics of GC through the Wnt/β-catenin pathway. Firstly, we determined the aberrant expression of ZNF710 in GC through public databases and a variety of basic experimental approaches. Subsequently, ZNF710 was overexpressed or knocked down in GC cells to observe the effect of ZNF710 on the cell biological behavior of GC. Furthermore, we hypothesized and validated the role of ZNF710 in the Wnt/β-catenin. Finally, we designed retrospective experiments and in vivo experiments, and combined both approaches to validate our conclusions.

Materials and methods

Clinical samples

Shanghai General Hospital's Department of Gastrointestinal Surgery provided 10 pairs of cancer and paracancerous tissues from GC patients. All patients had not undergone chemotherapy or neoadjuvant therapy prior to surgery, and the pathological reports were confirmed post-surgery. This study was reviewed and approved by the Ethics Committee of Shanghai General Hospital.

Cell culture and treatments

The Gastrointestinal Surgery Laboratory of Shanghai General Hospital supplied the cell lines required for this study, which included human normal gastric epithelial cells (GES-1) and human gastric cancer cells (AGS, MKN-28, and HGC-27). All cell lines used in the study were authenticated via short tandem repeat (STR) profiling. The cells were cultured in RPMI-1640 medium (BIOAGRIO, Shanghai, China) at 37°C in 5% CO_2.

Following transduction of the lentivirus for 16 h, puromycin was used to select transduced ZNF710 lentiviral overexpression (oeZNF710) and shRNA plasmids and vectors (shZNF710) cell lines, thereby establishing cell lines with stable expression.

In the present study, SKL2001 (Wnt activator) was used to increase the activity of the Wnt/β-catenin in GC cells (HGC-27 cells were treated with 40 μM SKL2001 for 24 h). While XAV939 (Wnt inhibitor) was used to decrease the activity of the Wnt/β-catenin in GC cells (AGS cells were treated with 10 μM XAV939 for 48 h).

Western blotting

Proteins were extracted from cells or tissues via RIPA buffer. The samples were transferred to polyvinylidene fluoride (PVDF) membrane by 10% SDS-PAGE electrophoresis. Membranes were incubated with the first antibody [ZNF710 (1:1000, #bs-4373R Bioss, Beijing, China), Wnt-1 (1:1000, #27935, Proteintech, CHI, USA), β-catenin (1:1000, #8480, CST, MA, USA), c-Myc (1:1000, #5605, CST), Cyclin D1 (1:1000, #55506, CST), β-actin (1:2000, Proteintech)] overnight, and the secondary antibody (1:10000) was added the next day.

Quantitative real-time polymerase chain reaction (qRT-PCR)

Total RNA was extracted by TRIzol (Thermo Fisher, Shanghai, China) and reverse transcribed according to kit instructions to obtain cDNA. This was followed by qRT-PCR analysis (**Table 1**).

Table 1. The sequences of the primers used for qRT-PCR

Gene	Forward primer (5'-3')	Reverse primer (5'-3')
ZNF710	AGTGTGACAAGTCCTTCCACTACC	GGTGGTGAATCTGGCTGAACTC
ACTIN	CACCATTGGCAATGAGCGGTTC	AGGTCTTTGCGGATGTCCACGT

CCK-8 assay

Cells were seeded in 96-well plates (3×10^3 cells/well) for 24 h. The absorbance value (450 nm) was detected by microplate reader.

Transwell migration assay

Resuspend the cells in 200 μl serum-free medium and seed them into the upper transwell chamber. Add a total of 600 μl of medium containing 10% FBS to the lower chamber. After 24 h of incubation, the transmembrane cells were fixed. Remove the paraformaldehyde solution, stained with 0.1% crystal violet for 10 min. Count the number of migrating cells in five different fields of view under an inverted microscope and take the average for comparison of the migration ability between different treatment groups.

Wound healing assay

The cells were seeded in a 24-well plate. A scratch area was constructed at the center of the plate using the tip of a 200 μl sterile pipette. Cell migration was calculated using ImageJ software.

Plate cloning experiment

Cells were inoculated in 6-well plates, and they must be adequately mixed to prevent the formation of cell clumps. Before placing the plate in the cell culture incubator, an 8-figure motion was used to distribute the cells evenly. After the occurrence of visible colonies in the six-well plate, end the culture. To quantify colony formation, remove the culture medium, and then add 1 mL of paraformaldehyde to each well and incubate for 20 min, stained with crystal violet. Subsequently, collect images and observe and quantify the number of visible colonies on the plate using ImageJ software.

Flow cytometric apoptosis assay

The cells (5×10^5) were digested, centrifuged, and resuspended in 300 μL of 1 × binding buffer. Annexin V-fluorescein isothiocyanate (Annexin V-FITC) and propidium iodide (PI) (Absin, Shanghai, China) were added sequentially. The apoptosis rate was detected by flow cytometry.

Flow cytometric cell cycle progression assay

Cells were seeded into 6-well plates and collected when they were in the logarithmic growth phase. The collected cells were washed with cold PBS twice and fixed in 95% ethanol for 24 h. The next day, 1 mg/mL PI dye was added for staining. Cell cycle was detected by flow cytometry. To further quantitatively assess cell proliferation activity, the Proliferation Index (PI, distinct from the PI dye used for staining) was calculated based on the phase distribution results. The Proliferation Index reflects the proportion of cells in proliferative phases (S and G2/M) relative to the total cell population.

GSEA-KEGG enrichment analysis

Using transcriptomic data from 415 primary tumor samples of TCGA-STAD database. Samples were stratified into ZNF710-high (n=208, expression > median) and ZNF710-low (n=207, expression ≤ median) groups; each gene's log2 fold change (log2FC, ZNF710-high vs. low) was calculated using mean TPM values (set to ≥ 0.00001 to avoid errors), and genes were preranked by descending log2FC. GSEA was implemented via the GSEA function in clusterProfiler package, with the MSigDB KEGG gene set ($P < 0.05$ considered significant).

Nude mouse xenograft model

Each BALB/c nude mouse (4-6 weeks) was injected subcutaneously with 5×10^6 GC cells from different treatment groups [purchased from Jiangsu Hengfengqiang Biotechnology Co., LTD., Animal use license number: SYXK (Su) 2024-0023]. After 3 weeks, the mice were euthanized by carbon dioxide (CO_2) inhalation (a special CO_2 euthanasia box was used, and the mice were placed into the box. The CO_2 concentration was slowly increased to 20% within

the initial 30 s, and then gradually increased to 30-50% within 5-10 min. When complete cessation of respiratory movement and pupil dilation were observed, the CO_2 concentration was maintained for at least 1 minute to ensure brain death), and the intact subcutaneous tumor tissue was removed. To compare the effects of different treatments on tumor growth, we measured tumor volume every five days and weighed tumors at the end of the experiment. The experiment was reviewed and approved by the Animal Care Committee of Shanghai General Hospital. The maximum tumor burden allowed by the animal ethics Committee of our hospital was 5% of the body weight of the animal, and all tumor mentions in this study met this criterion.

Immunohistochemical staining

Tumor tissue sections of nude mice were made. The antigen was retrieved at high temperature, and the primary antibody was incubated overnight with ZNF710 (1:200, #bs-4373R Bioss, Beijing, China) and Ki-67 (1:500, #GB111141, Servicebio, Wuhan, China) antibodies after blocking. The next day, the corresponding secondary antibody (#G1302, Servicebio, Wuhan, China) was incubated for 1 hour, followed by a chromogenic reaction using diaminobenzidine (DAB), and finally dehydrated and visualized with a microscope.

Statistical analysis

In this study, data were expressed as mean ± standard deviation (SD) for normally distributed continuous variables. The data were analyzed via GraphPad Prism 10 (GraphPad Software, MD, USA). Student's *t* test and one-way ANOVA were used for data analysis. Significant differences are indicated as follows: ns = not significant, *P < 0.05, **P < 0.01, ***P < 0.001, and ****P < 0.0001.

Results

Clinical significance of ZNF710 in GC

The results of Gene Expression Profiling Interactive Analysis (GEPIA2) indicated that ZNF710 was upregulated in GC (**Figure 1A**). Additionally, data from the TCGA database revealed that the transcriptional levels of ZNF710 were significantly greater in 415 GC tissues than in 34 nontumor gastric tissues (**Figure 1B**). The expression of ZNF710 in GC patients with different clinical parameters was analyzed via the UALCAN database. In addition, ZNF710 was elevated with tumor progression (**Figure 1C**). On the basis of the analysis of individual cancer stages, the expression of ZNF710 significantly differed across stages 1, 2, and 3 (Supplementary Figure 1A). Additionally, the results suggest that elevated expression of ZNF710 could be linked to lymph node metastasis (Supplementary Figure 1B). We subsequently validated the expression level of ZNF710 in the GEO database (GSE54129, GSE33335, and GSE27342) and found that its high expression in GC was statistically significant (**Figure 1D**, Supplementary Figure 1C, 1D).

Chromosome 15, where ZNF710 is located, shows a high GISTIC score, suggesting that the increase in copy number in this region may be related to the occurrence and development of GC and high expression of ZNF710 (**Figure 1E**). In GC, the 25% of samples with the highest expression of ZNF710 presented greater proportions of genomic changes, loss, and acquisition (Supplementary Figure 1E). In GC, a Spearman rank correlation coefficient of 0.35 was observed between the Gistic2-corrected copy number scores of ZNF710 and its corresponding mRNA expression levels, with a *p* value of 1.7e-13, indicating a significant positive correlation between these variables (**Figure 1F**). We further performed copy number spectroscopy (CNS) via a genome-wide microarray at the TCGA Genomic Characterization Center. The Gistic2 algorithm was subsequently applied through the TCGA FIREHOSE pipeline to generate copy number estimates at the gene level. The results revealed an overall increasing trend in ZNF710 expression levels, ranging from homozygous deletion to high copy number amplification (**Figure 1G**).

The expression levels of ZNF710 were significantly lower in samples with the Microsatellite Instability (MSI)-High subtype than in those with the MSI-Low and Microsatellite Stable subtypes (**Figure 1H**). Survival analysis showed that the overall survival (OS), progression-free survival (PFS) and post-progression survival (PPS) of GC patients with elevated expression of ZNF710 were poor, and all *P* values were less than 0.05 (**Figure 1I-K**).

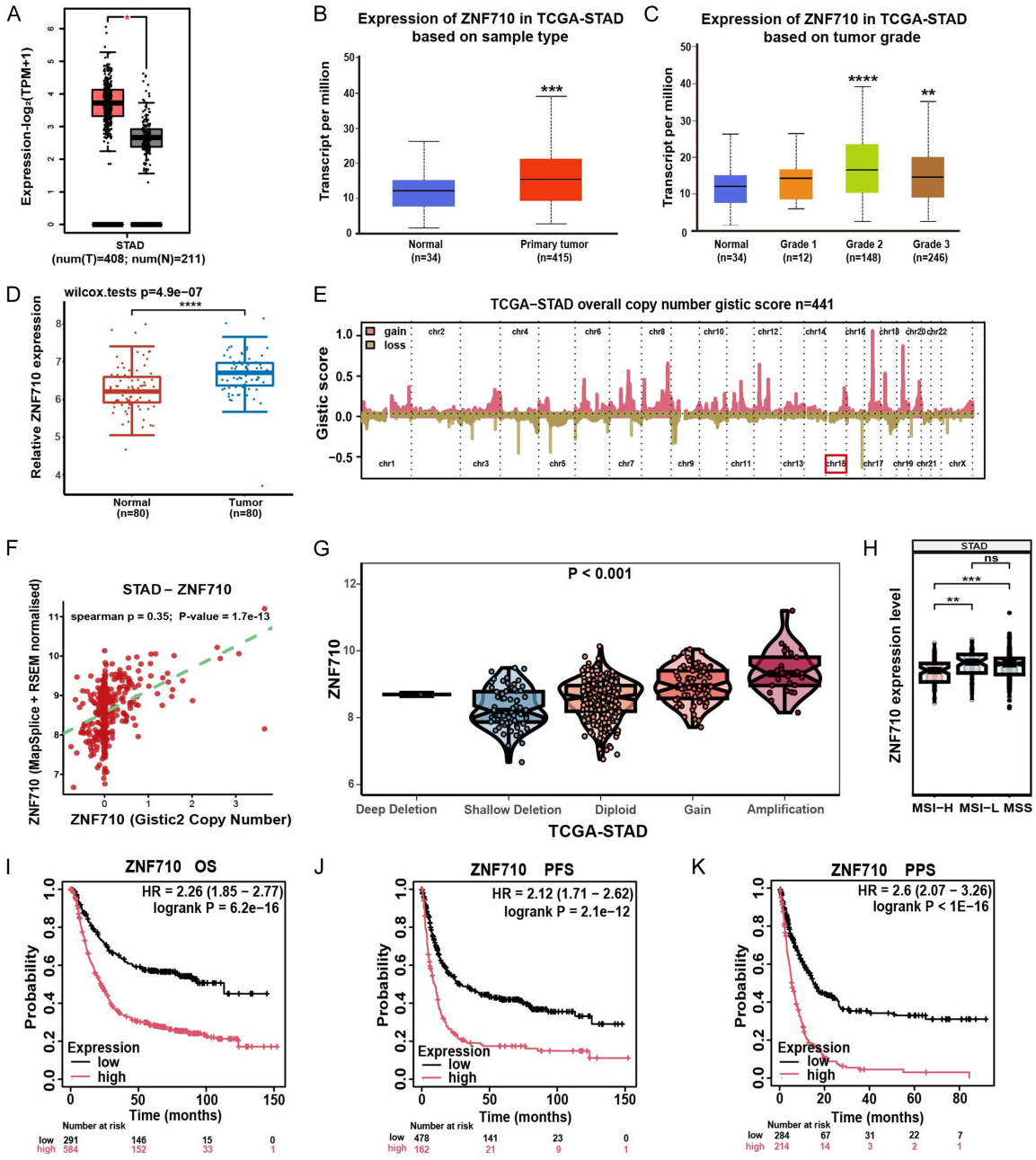

Figure 1. ZNF710 is overexpressed and associated with poor prognosis in GC patients. A. The Gene Expression Profiling Interactive Analysis (GEPIA2) database was utilized to investigate the expression levels of ZNF710 in GC. B. Analysis of ZNF710 expression levels in normal (n=34) and tumor (n=415) tissues in the TCGA database. C. ZNF710 expression levels were compared across patient groups with different tumor grades via the UALCAN database. D. ZNF710 expression in GC was further validated via the GEO database (GSE54129). E. Copy number variations in the genomes of 441 samples in the TCGA-STAD project. F. Spearman correlation between the CNV score and ZNF710 expression level. G. ZNF710 expression in different copy number variation subtypes. H. ZNF710 expression levels in different MSI subgroups of TCGA-STAD samples. I-K. The KM plotter database was used to investigate the prognostic impact of high ZNF710 expression on the overall survival (OS), progression-free survival (PFS) and post-progression survival (PPS) in patients with GC.

ZNF710 is upregulated in GC

ZNF710 exhibited a significantly increased expression profile in GC tissues when contrasted with normal tissues (**Figure 2A-E**). Relative to the GES-1 cell line, MKN-28 and HGC-27 cells displayed notably higher ZNF710 expression levels, with HGC-27 cells demonstrating

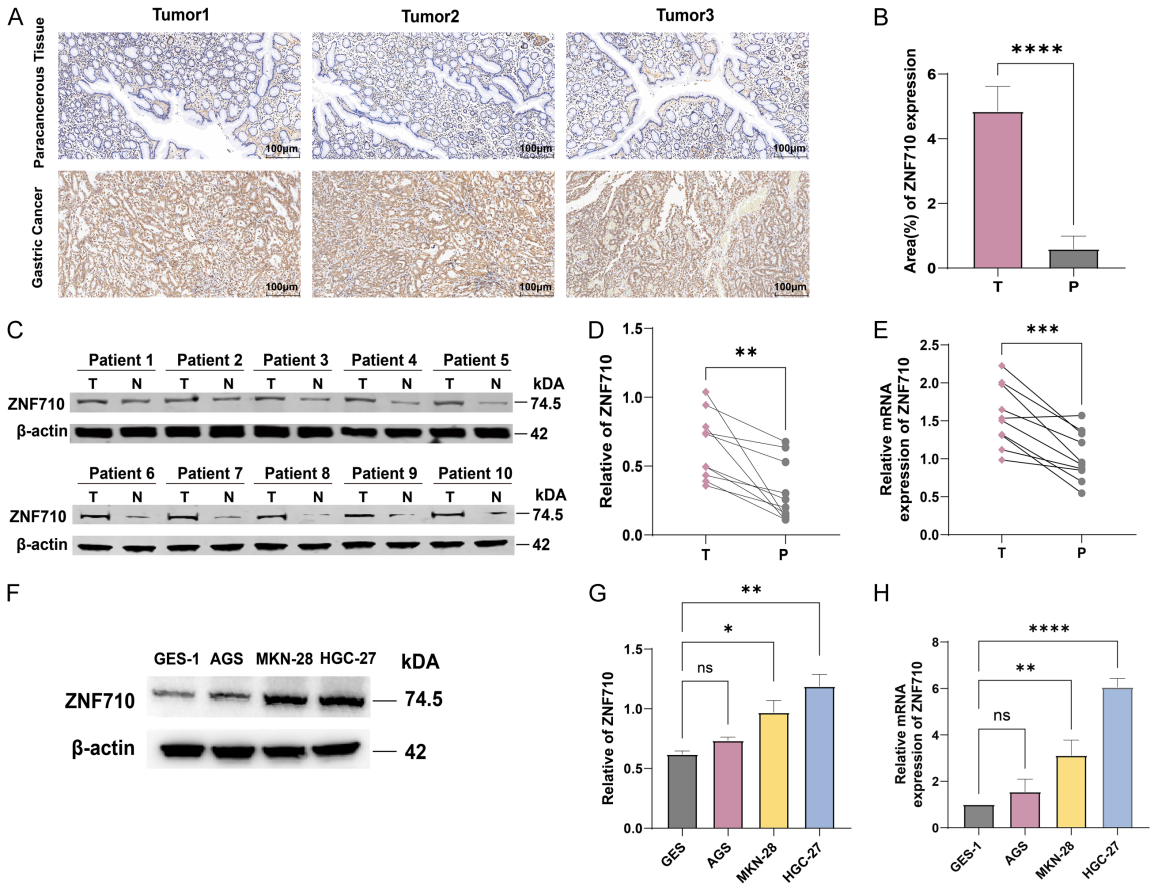

Figure 2. ZNF710 is upregulated in GC tissues and cell lines. (A, B) Representative images and analysis of ZNF710 immunohistochemical staining in 10 pairs of GC tissues and paracancerous tissues (scale bars: 100 μm, magnification: 200×). The relative levels of ZNF710 protein expression and mRNA transcripts in clinical human GC tissues and corresponding paracancerous tissues were analyzed by western blotting (C, D) and qRT-PCR (E), respectively (n=10). Relative levels of ZNF710 protein expression and mRNA transcripts in normal human epithelial cells and in three human GC cell lines, as determined by Western blotting (F, G) and qRT-PCR (H).

the peak expression and AGS cells showing the lowest level among these cell lines (**Figure 2F-H**).

ZNF710 promotes proliferation and migration of GC

For further research, the AGS cell line, with relatively low ZNF710 expression, was used to construct an overexpression cell line for investigative purposes. Conversely, the HGC-27 cell line, which presented the highest expression of ZNF710, was selected to establish a stable ZNF710 knockdown cell line. Western blotting and qRT-PCR validation results demonstrate that ZNF710 expression was significantly increased in the oeZNF710 group compared to the oeNC group (Supplementary Figure 2A-C). Compared with the shNC group, the expression of ZNF710 in the shZNF710 groups was significantly lower (Supplementary Figure 2D-F). Given the most pronounced knockdown effect of shZNF710-1, it was selected for subsequent functional studies.

Compared with the oeNC group, ZNF710 overexpression enhanced the proliferation of AGS cells (**Figure 3A**), whereas knockdown of ZNF710 significantly inhibited the proliferative capacity of HGC-27 cells (**Figure 3B**). Similarly, overexpression of ZNF710 promoted colony formation in AGS cells (**Figure 3C**, **3D**), whereas downregulation of ZNF710 restricted colony formation in HGC-27 cells (**Figure 3E**, **3F**). These results indicate that ZNF710 contributes to the proliferation of GC cells.

Compared with the control group, ZNF710 overexpression increased the invasive and migratory capabilities of AGS cells, whereas ZNF710

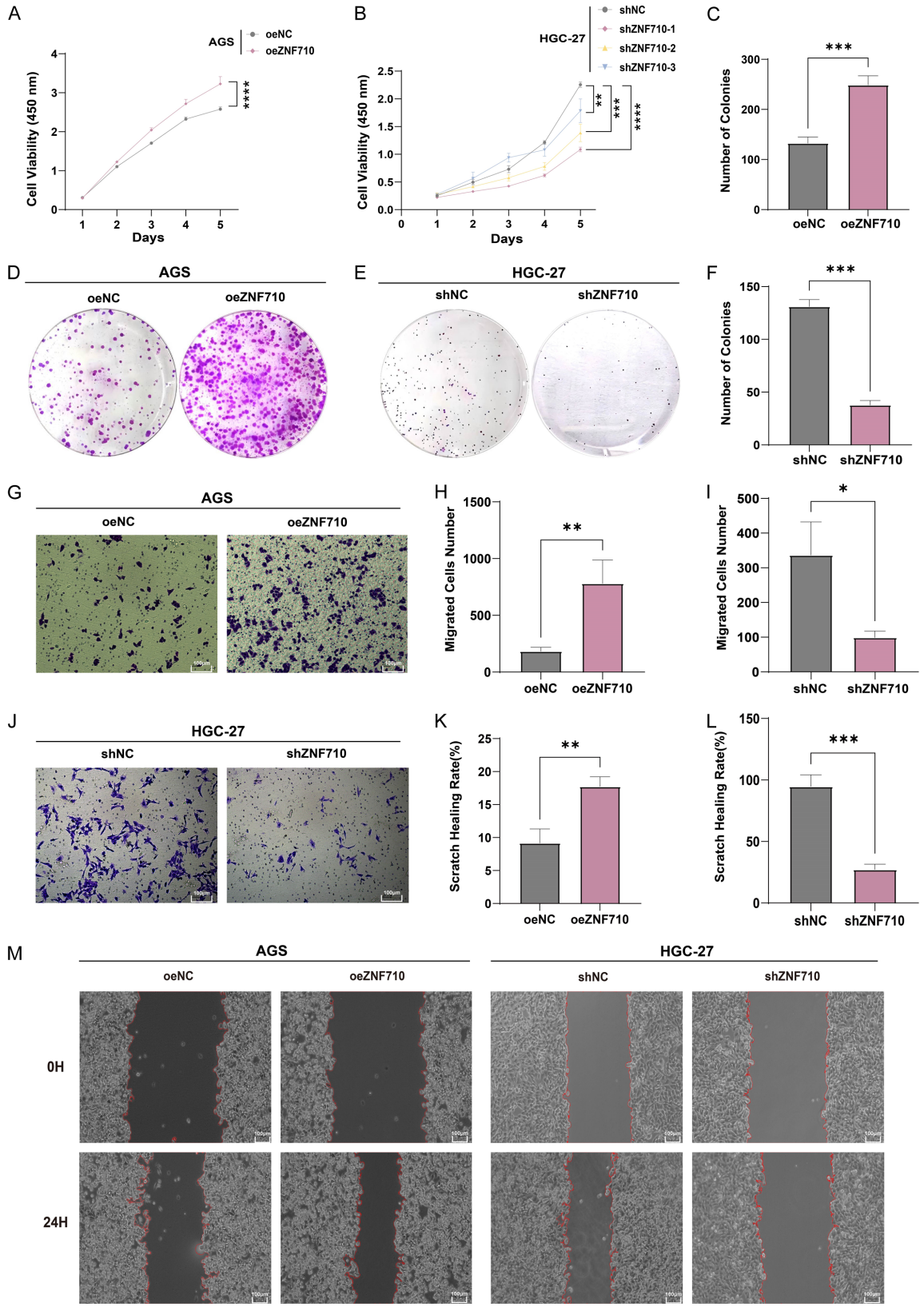

Figure 3. ZNF710 promotes proliferation and migration of GC. CCK-8 assay (A, B) and plate cloning experiment (C-F) were used to detect the proliferation ability of GC cells. Transwell migration assay (G-J, scale bars: 100 μm, magnification: 200×) and wound healing assay (K-M, scale bars: 100 μm, magnification: 100×) were used to detect the migration ability of GC cells.

downregulation markedly inhibited the invasive and migratory abilities of HGC-27 cells (**Figure 3G-M**).

ZNF710 inhibits apoptosis and promotes cell cycle progression in GC

Apoptosis analysis indicated that AGS cells transfected with oeZNF710 displayed a reduced apoptotic rate compared to the oeNC control group, while a converse trend was observed between the shZNF710 and shNC groups in HGC-27 cells (**Figure 4A-D**). Relative to shNC controls, ZNF710 knockdown significantly elevated the percentage of cells in the G0/G1 phase and diminished the proportion of S phase and G2M phase cells, with ZNF710 overexpression yielding opposing effects (**Figure 4E-H**).

ZNF710 promotes GC by activating the Wnt/β-catenin pathway

After GSEA-KEGG enrichment analysis of the TCGA data, we observed that upregulation of ZNF710 resulted in significant enrichment of the cell cycle and Wnt signaling pathway (**Figure 5A**). To visualize the expression pattern of Wnt pathway genes in association with ZNF710, we generated a heatmap of Wnt signaling-related genes in the TCGA cohort, stratified by ZNF710-high and ZNF710-low subgroups (**Figure 5B**). The heatmap clearly showed that core components of the Wnt/β-catenin pathway - including Wnt1, β-catenin, c-Myc, and Cyclin D1 - exhibited markedly higher expression in the ZNF710-high subgroup compared to the ZNF710-low subgroup. Moreover, by calculating and analyzing the Pearson correlation coefficients between genes in the TCGA dataset, the expression of ZNF710 was found to be positively correlated with the expression of Ki-67 and β-catenin (**Figure 5C**). Western blotting results revealed that ZNF710 overexpression significantly increased the protein expression of Wnt-1, β-catenin, c-Myc, and Cyclin D1 in AGS cells, whereas downregulation of ZNF710 decreased the expression of these proteins in HGC-27 cells (**Figure 5D**, **5E**).

We hypothesize that if Wnt agonists can reverse the previously observed effects of ZNF710 knockdown on cell proliferation and cell cycle progression, this would substantiate the positive regulatory role of ZNF710 on the Wnt/β-catenin. The results of the CCK-8 assay and plate cloning experiment revealed that the proliferative ability of shZNF710-HGC-27 cells treated with the Wnt signaling pathway agonist SKL2001 was restored (**Figure 5F-H**) while the proportion of cells in the S phase and G2M phase was increased (**Figure 5I-K**). To further validate this mechanism, AGS cells in the oeZNF710 and oeNC groups were treated with the Wnt signaling pathway inhibitor XAV939 to investigate whether it could reverse the effects on cell proliferation and cell cycle progression. The results of CCK-8 assay and colony formation assay showed that the proliferative capacity of oeZNF710-AGS cells treated with XAV939 was inhibited (Supplementary Figure 3A-C), and the proportion of cells in the S phase and G2M phase was decreased (Supplementary Figure 3D-F).

ZNF710 promotes GC growth in vivo

Tumors in the oeZNF710 group had larger volumes compared to the oeNC group. (**Figure 6A-C**), whereas the tumors in the shZNF710 group were smaller than those in the shNC group. Moreover, the tumors formed by SKL2001-treated cells were larger than those formed by the control cells (**Figure 6D-F**). The results of immunohistochemistry demonstrated that Ki-67 expression was greater in the oeZNF710-AGS group than in the oeNC-AGS group (**Figure 6G**), and the opposite was true for shZNF710-HGC-27 cells (**Figure 6H**). Furthermore, upon treatment with SKL2001, the expression of Ki-67 significantly increased. Thus, ZNF710 promotes the growth and proliferation of GC cells in vivo through the Wnt/β-catenin.

Discussion

In recent years, the association between zinc finger proteins and GC has attracted wide attention in the world, involving cellular immune cell infiltration, DNA methylation patterns and other aspects [21-25]. However, the specific mechanisms by which ZNF710 influences cancer development remain unclear. Therefore, we specifically investigated the downstream mechanisms by which ZNF710 promotes GC development, and we have indeed found evidence demonstrating that ZNF710 enhances GC progression by enhancing the Wnt/β-catenin in this study.

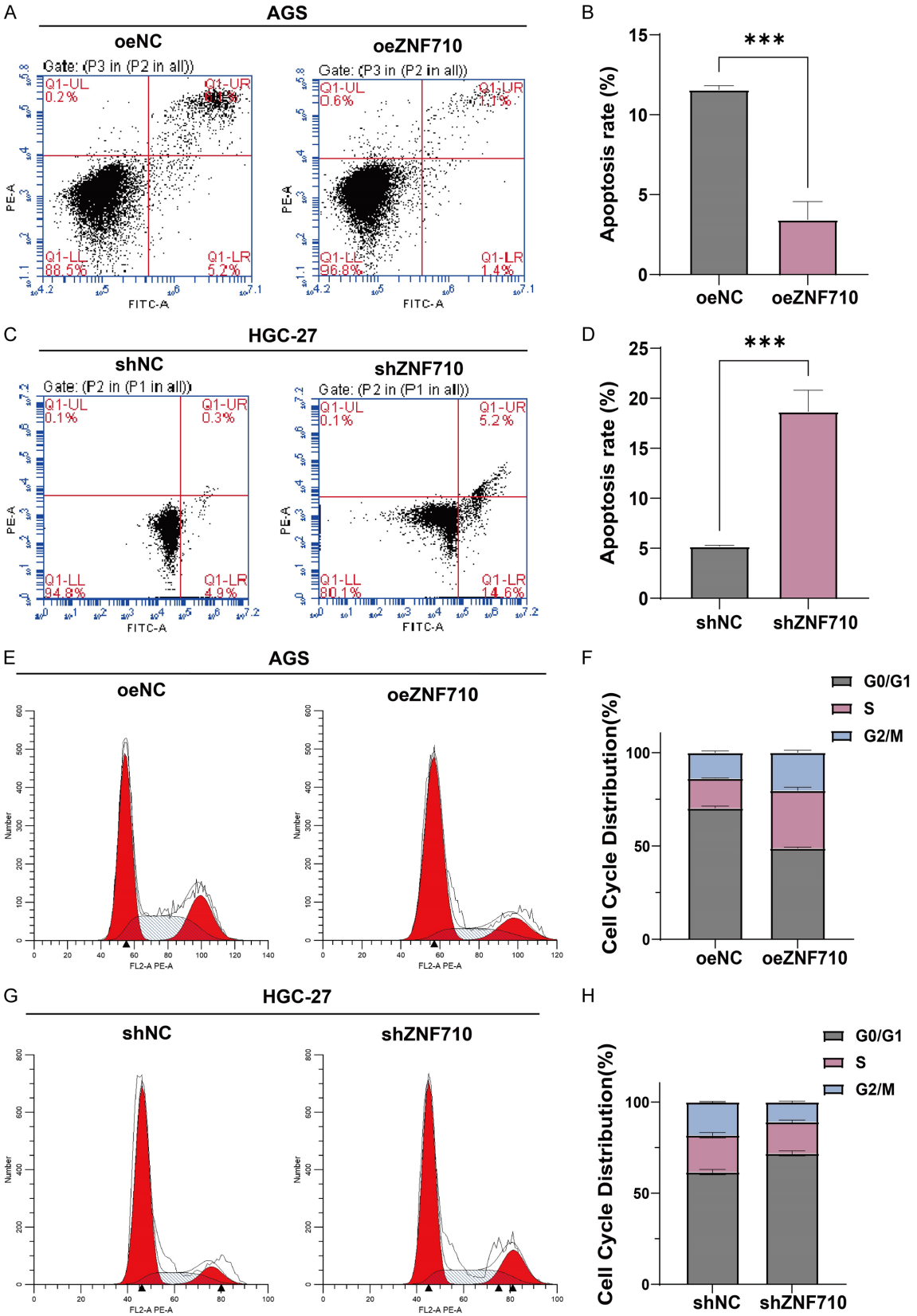

Figure 4. ZNF710 inhibits apoptosis and promotes cell cycle progression in GC. A-D. The apoptosis rates of AGS and HGC-27 cells were detected via flow cytometry. E-H. Cell cycle progression of AGS and HGC-27 cells was detected by flow cytometry.

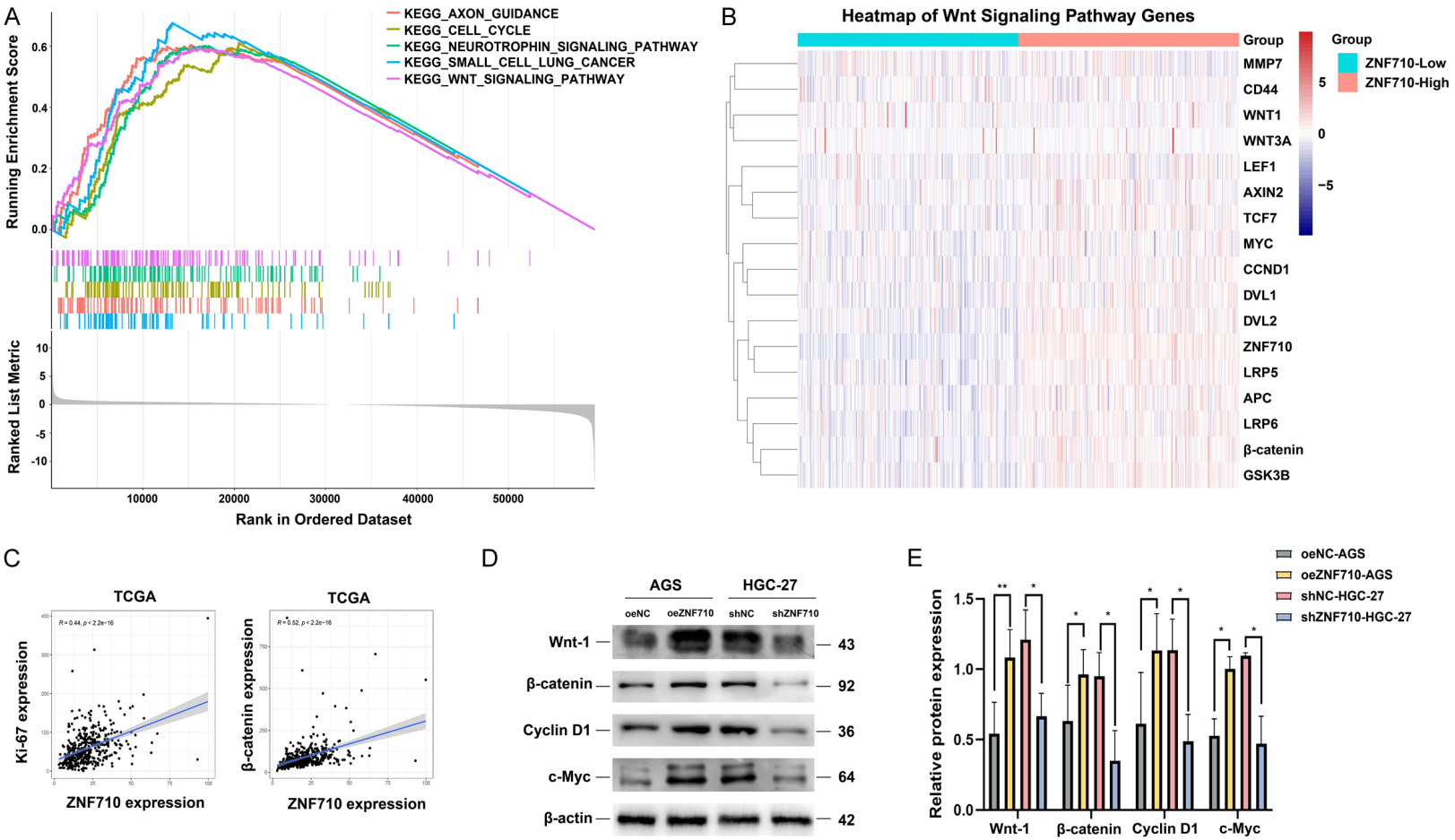
A
KEGG_AXON_GUIDANCE
KEGG_CELL_CYCLE
KEGG_NEUROTROPHIN_SIGNALING_PATHWAY
KEGG_SMALL_CELL_LUNG_CANCER
KEGG_WNT_SIGNALING_PATHWAY
Running Enrichment Score
Ranked List Metric
Rank in Ordered Dataset
B
Heatmap of Wnt Signaling Pathway Genes
Group
ZNF710-Low
ZNF710-High
MMP7
CD44
WNT1
WNT3A
LEF1
AXIN2
TCF7
MYC
CCND1
DVL1
DVL2
ZNF710
LRP5
APC
LRP6
β-catenin
GSK3B
C
TCGA
Ki-67 expression
ZNF710 expression
TCGA
β-catenin expression
ZNF710 expression
D
AGS
HGC-27
oeNC
oeZNF710
shNC
shZNF710
Wnt-1
β-catenin
Cyclin D1
c-Myc
β-actin
43
92
36
64
42
E
oeNC-AGS
oeZNF710-AGS
shNC-HGC-27
shZNF710-HGC-27
Relative protein expression
Wnt-1
β-catenin
Cyclin D1
c-Myc

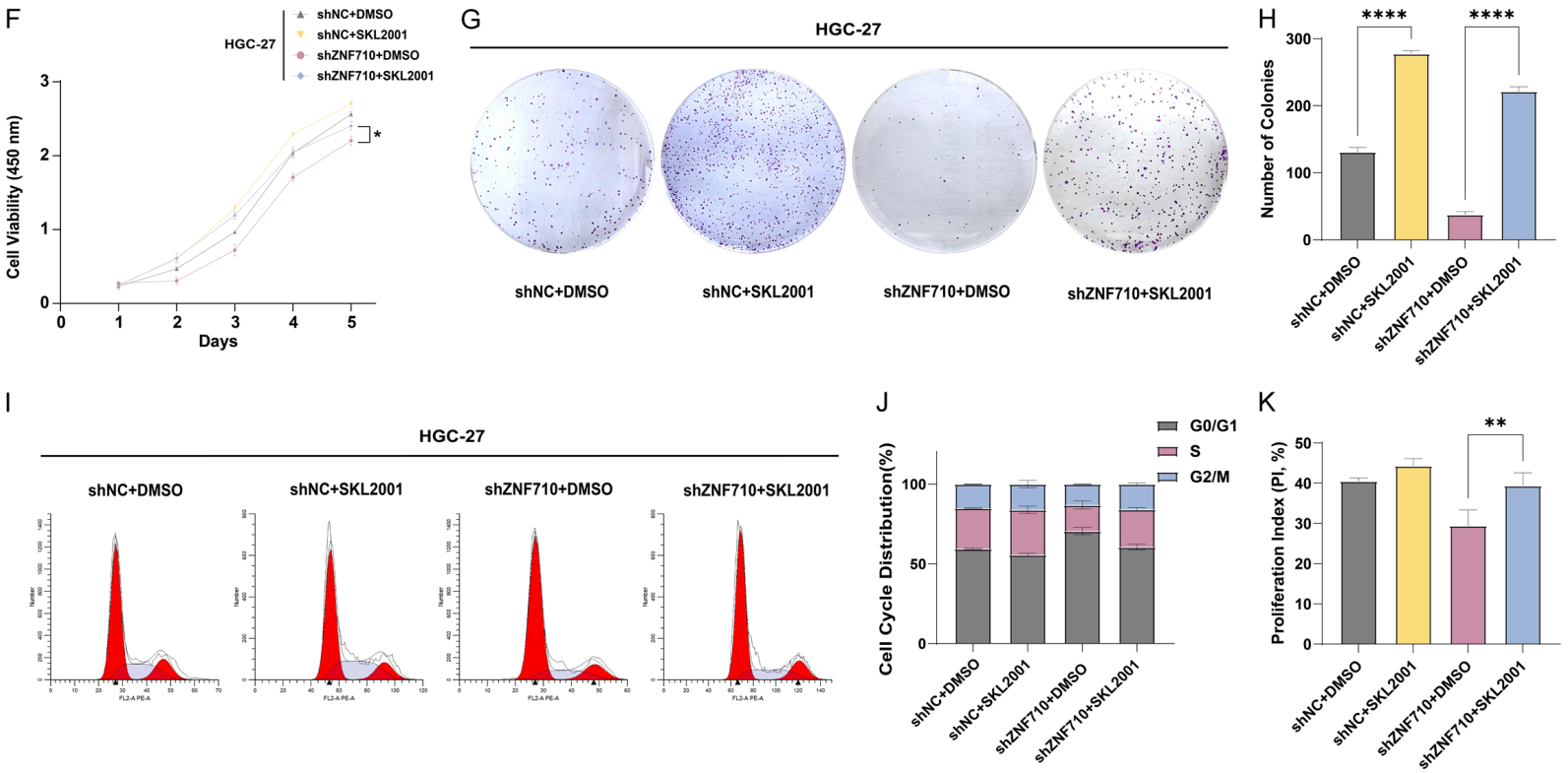

Figure 5. ZNF710 promotes GC by activating the Wnt/β-catenin pathway. A. GSEA-KEGG enrichment analysis of TCGA data. B. Heatmap showed the expression profile of Wnt signaling pathway-related genes in the ZNF710-high and ZNF710-low groups. C. Correlations between ZNF710 and Ki-67 and β-catenin mRNA expression in the TCGA dataset. D, E. Western blotting was used to analyze the expression of Wnt-1, β-catenin, and cyclin-related proteins proteins (c-Myc and cyclin D1) in oeZNF710 cells and shZNF710 cells. F-H. The restoration of HGC-27 cell proliferation capacity induced by SKL2001 was analyzed via CCK-8 assay and plate cloning experiment. I-K. Changes in the cell cycle progression of HGC-27 cells following treatment with SKL2001 were detected by flow cytometry.

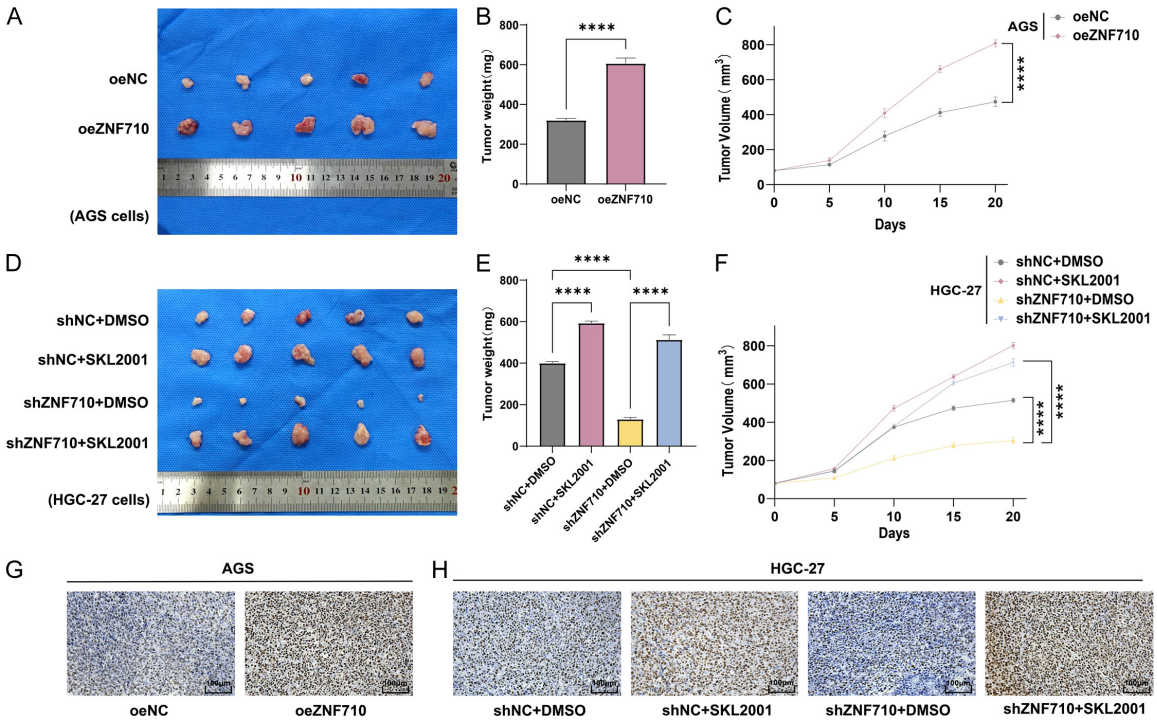

Figure 6. ZNF710 promotes GC growth in vivo. A-F. Images of subcutaneous tumor formation in nude mice injected with AGS and HGC-27 cells from different treatment groups (*n*=5 for each group). G, H. Representative Ki-67 staining images of paraffin-embedded subcutaneous tumor sections (scale bars: 100 μm, magnification: 200×).

In previous studies on zinc finger proteins, researchers identified differentially expressed genes, including those of the zinc finger family, via the use of public databases and visualized them via Venn diagrams and heatmaps [26]. In the bioinformatics section of our study, we performed a comprehensive analysis of ZNF710 using multiple public databases. Our analysis focused on expression levels and patient prognosis, leading to the conclusion that ZNF710 is highly expressed in GC.

High mortality rates among cancer patients are primarily attributed to the invasive and metastatic properties of tumors. The members of the zinc finger protein family, including ZNF521 and ZNF460 appear to be the primary contributors to the malignancy of GC by influencing its proliferation and migration [27, 28]. In our study, multiple functional experiments further revealed that ZNF710 promotes the proliferation and migration of GC. Provided that the increased tumour migration ability provided by ZNF710 can be successfully suppressed, this will probably result in a favourable patient prognosis and survival rates. Therefore, downregulating ZNF710 can prevent GC.

Tumour cells, in comparison to normal cells, tend to lose control of their cell cycle, and cell cycle arrest is a newer approach towards treatment [29, 30]. In our study, we found that the cell cycle was suppressed when ZNF710 expression was downregulated, and the reverse was true. Even though ZNF710 inhibition has the potential to prevent the cell cycle in GC, how exactly ZNF710 facilitates the cell cycle process is a matter of study. Future studies could specifically explore the effects of ZNF710 and its downstream genes on cell cycle checkpoints, such as the G1/S transition.

Past literature has demonstrated that members of the zinc finger protein family determine tumor characteristics through the regulation of canonical signalling pathways [31]. In our study, we conducted bioinformatics analysis using ZNF710 expression as a starting point for GSEA in the TCGA database. The five most significantly enriched items included the cell cycle and the Wnt signaling pathway. Based on the experiences of other researchers, the Wnt/β-catenin pathway facilitates tumorigenesis and progression through the enhancement of cell proliferation, prevention of apoptosis, and the develop-

ment of stem-like properties in cells [32-34]. Overexpression of ZNF710 activated the expression of Wnt-1 and β-catenin in GC cells. Retrospective experiments using the Wnt agonist SKL2001 and Wnt inhibitor XAV939 further demonstrated that ZNF710 is related to the Wnt/β-catenin and influences the biological characteristics of GC.

Based on the results obtained above, we conducted an extensive study of ZNF710, examining its impact on metabolism and tumour immunity. We observed that most metabolic pathways were upregulated in the ZNF710 high expression group (Supplementary Figure 4A). The results demonstrated that in GC, ZNF710 expression was negatively correlated with the TIP scores of the cancer-immunity cycle (Supplementary Figure 4B). These results collectively confirm the oncogenic role of ZNF710 in promoting GC growth and provide insights for further investigations into the specific mechanisms by which ZNF710 regulates GC development.

However, our study also has some limitations, as we did not identify a direct relationship between ZNF710 and the Wnt/β-catenin. Although we speculate that there may be downstream genes of ZNF710 that directly influence the Wnt/β-catenin, direct evidence has yet to be identified. Additionally, our experimental procedures did not involve the use of transgenic mice or the construction of high-quality models, which is an area for further research. In the future, we plan to increase the experimental sample size, perform RNA sequencing. Additionally, we will actively investigate other potential mechanisms by which ZNF710 may influence GC, including its effects on immune cell infiltration and chemoresistance.

Conclusion

ZNF710 is a transcription factor that possesses the ability to promote the growth and invasion of GC. In GC, high expression of ZNF710 promotes tumor cell viability, by enhancing the Wnt/β-catenin.

Acknowledgements

We thank Mengkai Yang, Jun Zhang and Yichen Zhang from the Shanghai General Hospital for their valuable comments. This study was supported by the National Natural Science Foundation of China (81972215 to Yugang Wen) and the Interdisciplinary Program of Shanghai Jiao Tong University (YG2022QN069 to Yang Yu). Written informed consent was obtained from all participants or their legal guardians prior to their enrollment in the study.

Disclosure of conflict of interest

None.

Address correspondence to: Yugang Wen and Yang Yu, Department of General Surgery, Shanghai General Hospital, Shanghai Jiao Tong University School of Medicine, 85 Wujin Road, Shanghai 200080, China. E-mail: wenyg1502sjtu@163.com (YGW); Shmuyuyang@163.com (YY); Qi Li, Department of Oncology, Shanghai General Hospital, Shanghai Jiao Tong University School of Medicine, 85 Wujin Road, Shanghai 200080, China. E-mail: leeqi@sjtu.edu.cn

References

[1] Siegel RL, Kratzer TB, Giaquinto AN, Sung H and Jemal A. Cancer statistics, 2025. CA Cancer J Clin 2025; 75: 10-45.

[2] López MJ, Carbajal J, Alfaro AL, Saravia LG, Zanabria D, Araujo JM, Quispe L, Zevallos A, Buleje JL, Cho CE, Sarmiento M, Pinto JA and Fajardo W. Characteristics of gastric cancer around the world. Crit Rev Oncol Hematol 2023; 181: 103841.

[3] Chen YC, Malfertheiner P, Yu HT, Kuo CL, Chang YY, Meng FT, Wu YX, Hsiao JL, Chen MJ, Lin KP, Wu CY, Lin JT, O'Morain C, Megraud F, Lee WC, El-Omar EM, Wu MS and Liou JM. Global prevalence of helicobacter pylori infection and incidence of gastric cancer between 1980 and 2022. Gastroenterology 2024; 166: 605-619.

[4] Mok JW, Oh YH, Magge D and Padmanabhan S. Racial disparities of gastric cancer in the USA: an overview of epidemiology, global screening guidelines, and targeted screening in a heterogeneous population. Gastric Cancer 2024; 27: 426-438.

[5] Sundar R, Nakayama I, Markar SR, Shitara K, van Laarhoven HWM, Janjigian YY and Smyth EC. Gastric cancer. Lancet 2025; 405: 2087-2102.

[6] Ilic M and Ilic I. Epidemiology of stomach cancer. World J Gastroenterol 2022; 28: 1187-1203.

[7] Guan WL, He Y and Xu RH. Gastric cancer treatment: recent progress and future perspectives. J Hematol Oncol 2023; 16: 57.

[8] Bianchi D, Borza R, De Zan E, Huelsz-Prince G, Gregoricchio S, Dekker M, Fish A, Mazouzi A, Kroese LJ, Linder S, Hernandez-Quiles M, Vermeulen M, Celie PHN, Krimpenfort P, Song JY, Zwart W, Wessels L, Nijman SMB, Perrakis A and Brummelkamp TR. Zincore, an atypical coregulator, binds zinc finger transcription factors to control gene expression. Science 2025; 389: eadv2861.

[9] Gosztyla ML, Zhan L, Olson S, Wei X, Naritomi J, Nguyen G, Street L, Goda GA, Cavazos FF, Schmok JC, Jain M, Uddin Syed E, Kwon E, Jin W, Kofman E, Tankka AT, Li A, Gonzalez V, Lécuyer E, Dominguez D, Jovanovic M, Graveley BR and Yeo GW. Integrated multi-omics analysis of zinc-finger proteins uncovers roles in RNA regulation. Mol Cell 2024; 84: 3826-3842, e3828.

[10] Zhao J, Wen D, Zhang S, Jiang H and Di X. The role of zinc finger proteins in malignant tumors. FASEB J 2023; 37: e23157.

[11] Liu S, Liu X, Lin X and Chen H. Zinc finger proteins in the war on gastric cancer: molecular mechanism and clinical potential. Cells 2023; 12: 1314.

[12] Sun M, Ju J, Ding Y, Zhao C and Tian C. The signaling pathways regulated by KRAB zinc-finger proteins in cancer. Biochim Biophys Acta Rev Cancer 2022; 1877: 188731.

[13] Zhang L, Huo Q, Ge C, Zhao F, Zhou Q, Chen X, Tian H, Chen T, Xie H, Cui Y, Yao M, Li H and Li J. ZNF143-mediated H3K9 trimethylation upregulates CDC6 by activating MDIG in hepatocellular carcinoma. Cancer Res 2020; 80: 2599-2611.

[14] Li G, Xie M, Huang Z, Li H, Li P, Zhang Z, Ding Y, Jia Z and Yang J. Overexpression of antisense long non-coding RNA ZNF710-AS1-202 promotes cell proliferation and inhibits apoptosis of clear cell renal cell carcinoma via regulation of ZNF710 expression. Mol Med Rep 2020; 21: 2502-2512.

[15] Ding W, Chen WW, Wang YQ, Xu XZ, Wang YB, Yan YM and Tan YL. Immune-related long noncoding RNA zinc finger protein 710-AS1-201 promotes the metastasis and invasion of gastric cancer cells. World J Gastrointest Oncol 2024; 16: 458-474.

[16] Parsons MJ, Tammela T and Dow LE. WNT as a driver and dependency in cancer. Cancer Discov 2021; 11: 2413-2429.

[17] Zhao H, Ming T, Tang S, Ren S, Yang H, Liu M, Tao Q and Xu H. Wnt signaling in colorectal cancer: pathogenic role and therapeutic target. Mol Cancer 2022; 21: 144.

[18] Wu Q, Ma J, Wei J, Meng W, Wang Y and Shi M. lncRNA SNHG11 promotes gastric cancer progression by activating the Wnt/β-catenin pathway and oncogenic autophagy. Mol Ther 2021; 29: 1258-1278.

[19] Luan F, Li X, Cheng X, Huangfu L, Han J, Guo T, Du H, Wen X and Ji J. TNFRSF11B activates Wnt/β-catenin signaling and promotes gastric cancer progression. Int J Biol Sci 2020; 16: 1956-1971.

[20] Wang Y, Zheng L, Shang W, Yang Z, Li T, Liu F, Shao W, Lv L, Chai L, Qu L, Xu Q, Du J, Liang X, Zeng J and Jia J. Wnt/beta-catenin signaling confers ferroptosis resistance by targeting GPX4 in gastric cancer. Cell Death Differ 2022; 29: 2190-2202.

[21] Gao H, Li P, Hei Y, Li S, Wang J, Lv X and Zhang J. Long non-coding RNA-ZNF281 promotes cancer cell migration and invasion in gastric cancer via downregulation of microRNA-124. Oncol Lett 2020; 19: 1849-1855.

[22] Hong K, Yang Q, Yin H, Wei N, Wang W and Yu B. Comprehensive analysis of ZNF family genes in prognosis, immunity, and treatment of esophageal cancer. BMC Cancer 2023; 23: 301.

[23] Oleksiewicz U, Machnik M, Sobocińska J, Molenda S, Olechnowicz A, Florczak A, Smolibowski M and Kaczmarek M. ZNF714 supports pro-oncogenic features in lung cancer cells. Int J Mol Sci 2023; 24: 15530.

[24] O'Sullivan J, Kothari C, Caron MC, Gagné JP, Jin Z, Nonfoux L, Beneyton A, Coulombe Y, Thomas M, Atalay N, Meng XW, Milano L, Jean D, Boisvert FM, Kaufmann SH, Hendzel MJ, Masson JY and Poirier GG. ZNF432 stimulates PARylation and inhibits DNA resection to balance PARPi sensitivity and resistance. Nucleic Acids Res 2023; 51: 11056-11079.

[25] Barzegar S and Pirouzpanah S. Zinc finger proteins and ATP-binding cassette transporter-dependent multidrug resistance. Eur J Clin Invest 2024; 54: e14120.

[26] Wei J, Tan F, Long X, Fang Q, Wang Y, Wang J, He J, Yuan X and Du J. RNA-Seq transcriptome analysis of renal tissue from spontaneously hypertensive rats revealed renal protective effects of dapagliflozin, an inhibitor of sodium-glucose cotransporter 2. Eur J Pharm Sci 2023; 189: 106531.

[27] Huan C, Xiaoxu C and Xifang R. Zinc finger protein 521, negatively regulated by microRNA-204-5p, promotes proliferation, motility and invasion of gastric cancer cells. Technol Cancer Res Treat 2019; 18: 1533033819874783.

[28] An L and Liu Y. ZNF460 mediates epithelial-mesenchymal transition to promote gastric cancer progression by transactivating APOC1 expression. Exp Cell Res 2023; 422: 113452.

[29] Liu J, Zhang Q, Ruan B, Chen W, Zheng J, Xu B, Jiang P, Miao Z, Li F, Guo JY, Cao L and Wang G. MORC2 regulates C/EBPα-mediated cell differ-

entiation via sumoylation. Cell Death Differ 2019; 26: 1905-1917.
[30] Glaviano A, Singh SK, Lee EHC, Okina E, Lam HY, Carbone D, Reddy EP, O'Connor MJ, Koff A, Singh G, Stebbing J, Sethi G, Crasta KC, Diana P, Keyomarsi K, Yaffe MB, Wander SA, Bardia A and Kumar AP. Cell cycle dysregulation in cancer. Pharmacol Rev 2025; 77: 100030.
[31] Hou J, Huang P, Lan C, Geng S, Xu M, Liu Y, Chang H, Wang Z, Gu H, Wang Y, Yang G and Cui H. ZC3H15 promotes gastric cancer progression by targeting the FBXW7/c-Myc pathway. Cell Death Discov 2022; 8: 32.
[32] Han R, Yang J, Zhu Y and Gan R. Wnt signaling in gastric cancer: current progress and future prospects. Front Oncol 2024; 14: 1410513.
[33] Nie X, Wang H, Wei X, Li L, Xue T, Fan L, Ma H, Xia Y, Wang YD and Chen WD. LRP5 promotes gastric cancer via activating canonical Wnt/β-catenin and glycolysis pathways. Am J Pathol 2022; 192: 503-517.
[34] Li Y, Liu C, Zhang X, Huang X, Liang S, Xing F and Tian H. CCT5 induces epithelial-mesenchymal transition to promote gastric cancer lymph node metastasis by activating the Wnt/β-catenin signalling pathway. Br J Cancer 2022; 126: 1684-1694.

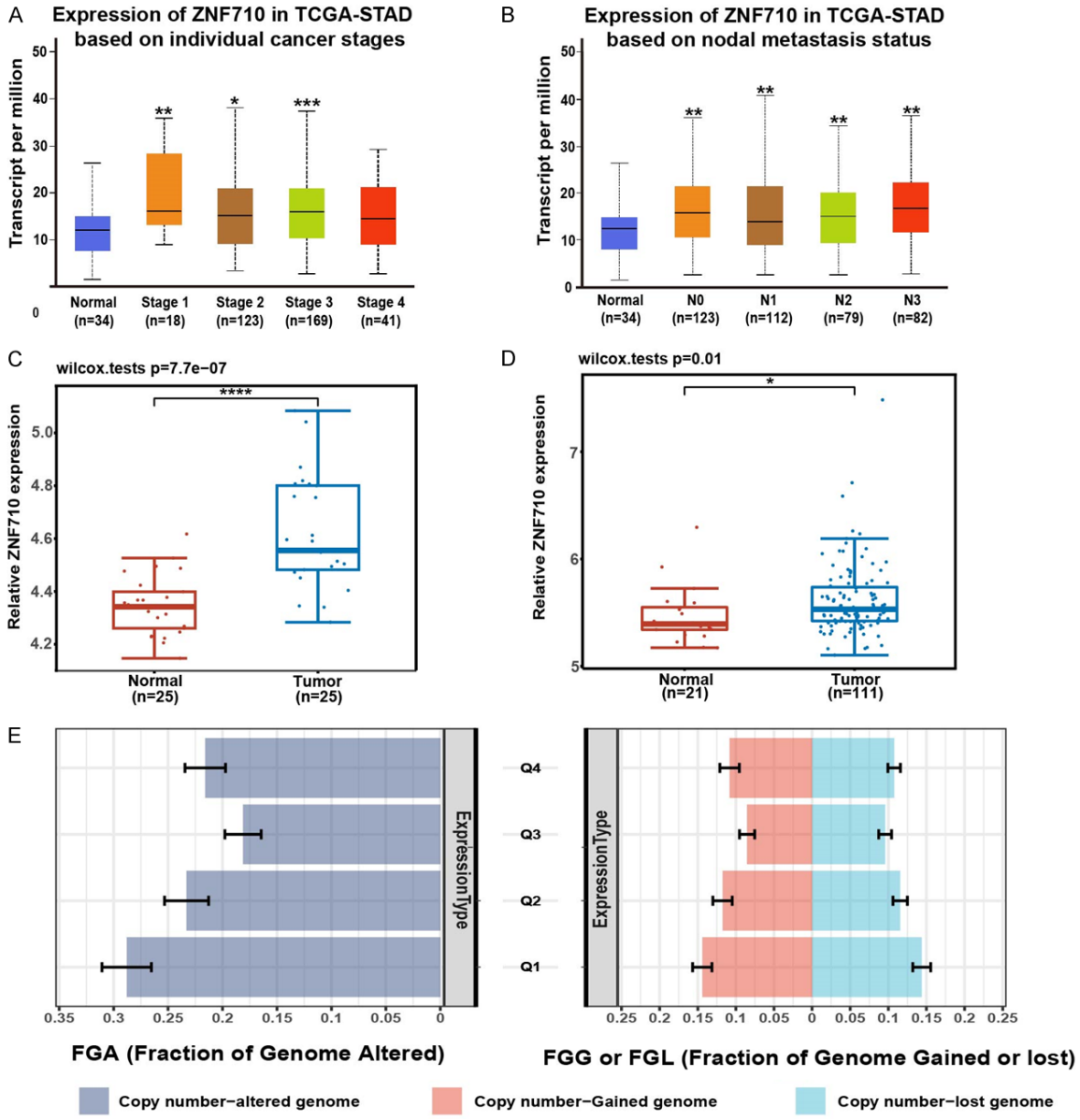

Supplementary Figure 1. Further validation of the aberrant expression of ZNF710 in GC. A, B. ZNF710 expression levels were compared across patient groups with different cancer stages and degrees of lymph node metastasis. C, D. The expression of ZNF710 in GC was further validated via the GEO database (GSE27342 and GSE33335). E. Percentages of FGL, FGG, and FGA in ZNF710 expression subsets for GC.

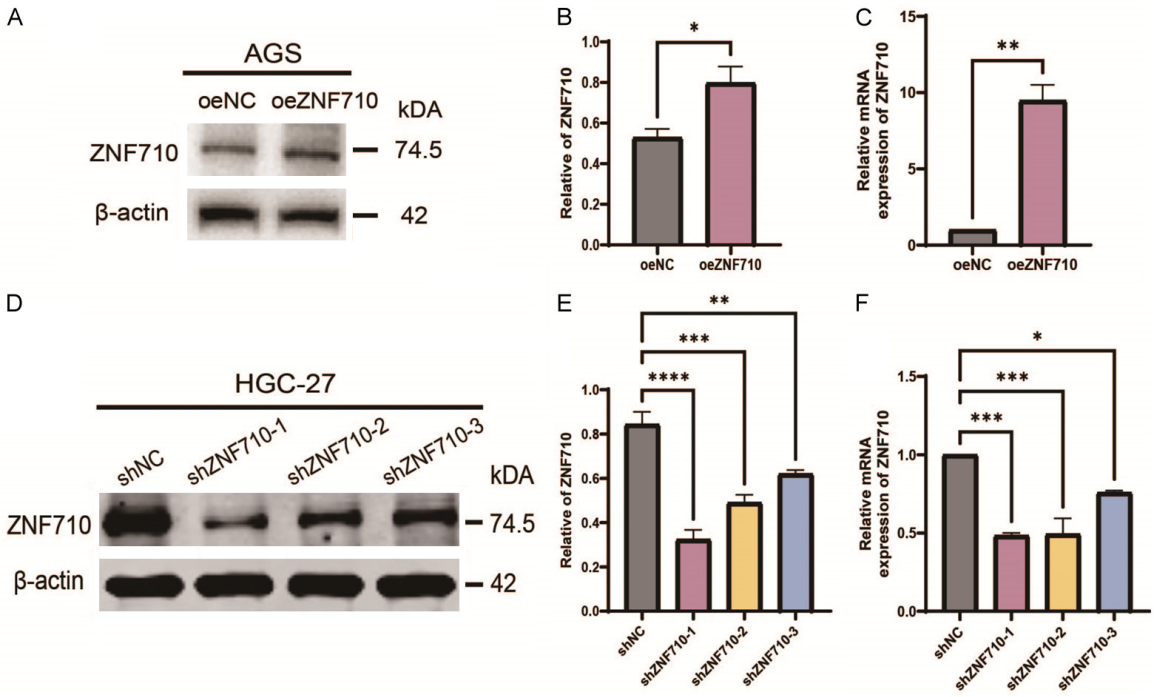

Supplementary Figure 2. Validation of lentivirus-mediated stable transfection. A-C. The relative levels of protein expression and mRNA transcripts verified ZNF710 overexpression in AGS cells. D-F. The relative protein expression and mRNA transcript levels confirmed the knockdown of ZNF710 in HGC-27 cells.

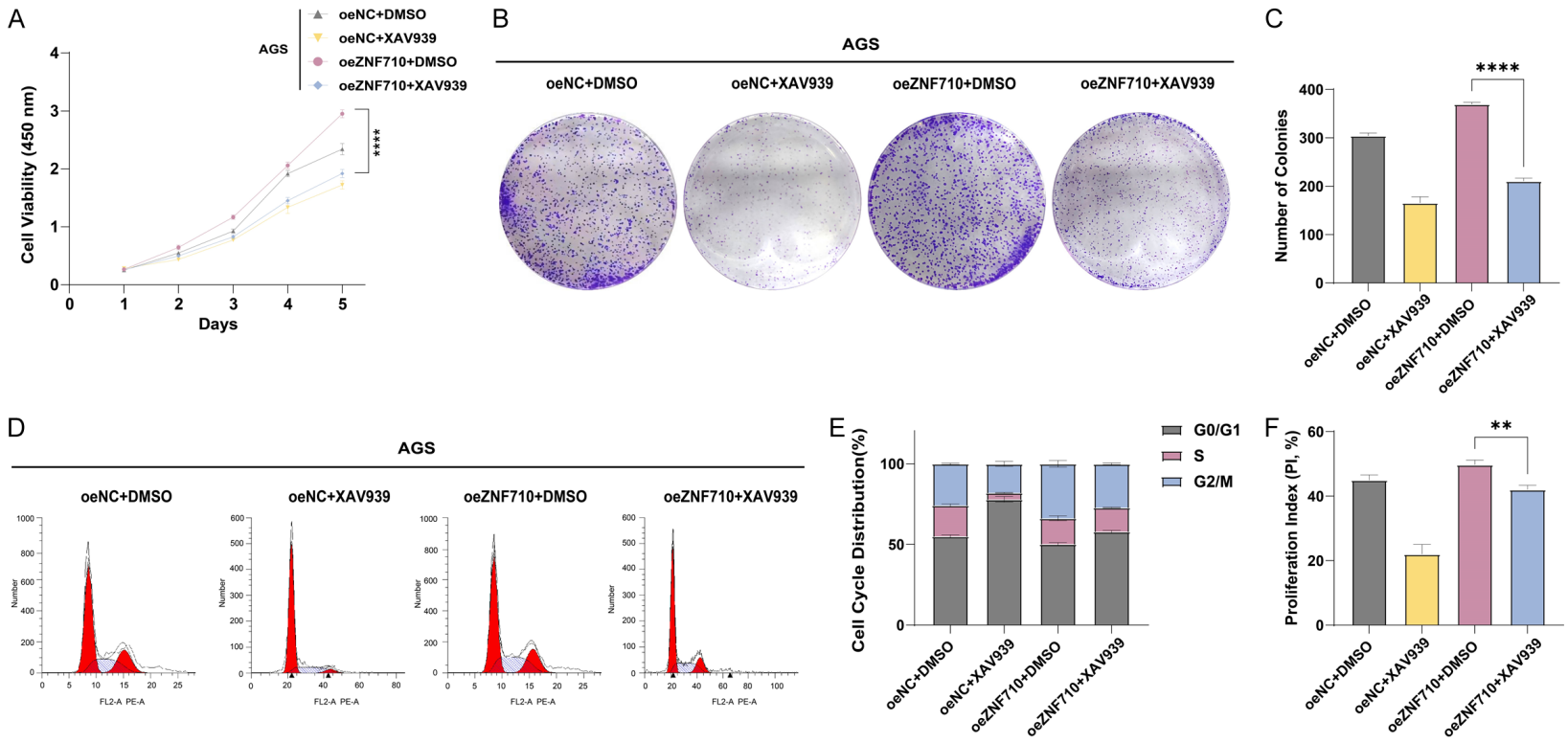

Supplementary Figure 3. Effect of the Wnt pathway inhibitor XAV939 on AGS cells. A-C. Effect of treatment with XAV939 on the proliferative capacity of AGS cells. D-F. Effect of treatment with XAV939 on the cell cycle progression of AGS cells.

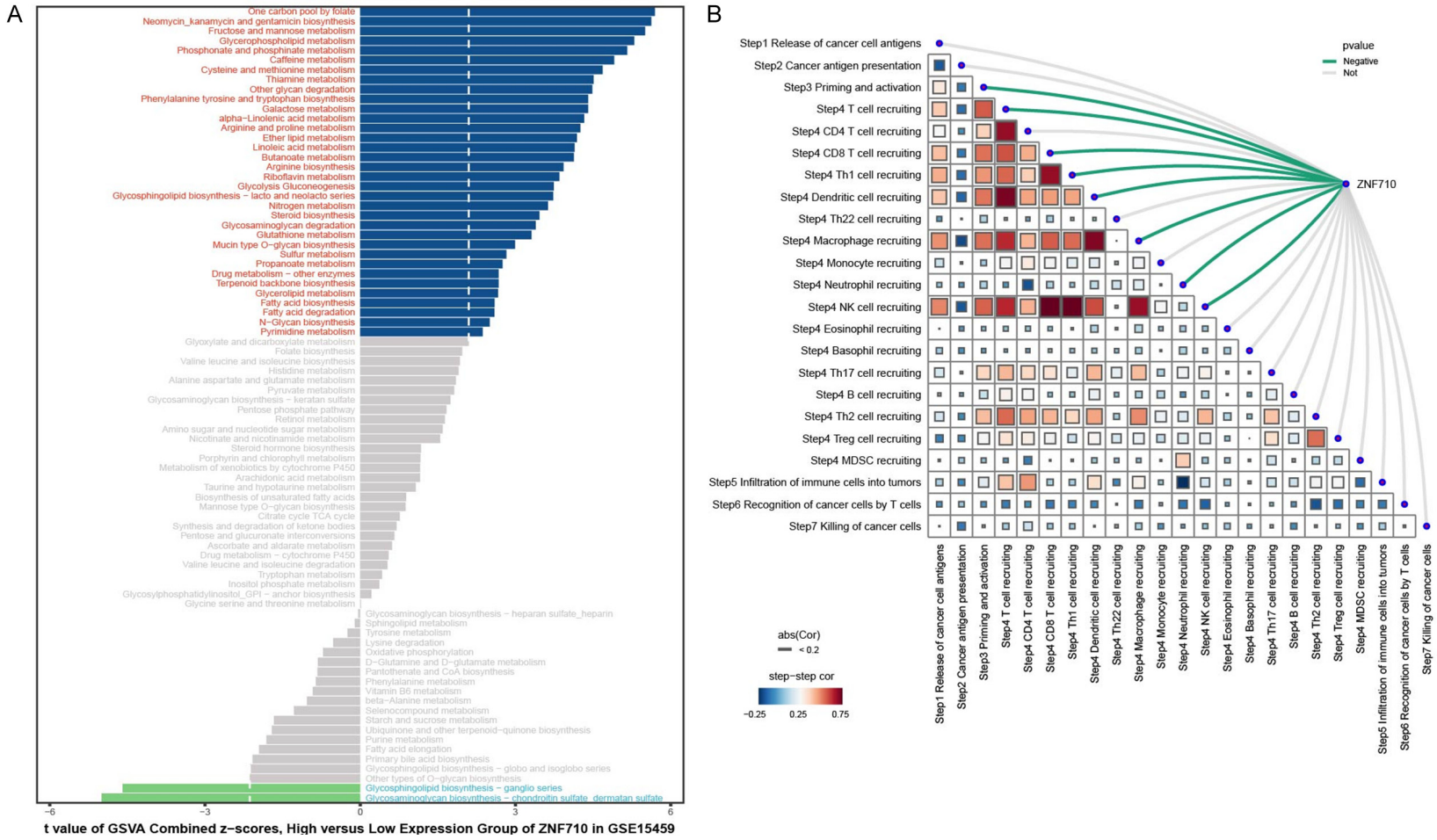

Supplementary Figure 4. Impact of ZNF710 expression on metabolic pathways and tumor immunity in GC. A. Differences in metabolic pathway GSVA scores between the high- and low-gene expression groups. B. Spearman correlation between the TIP score and ZNF710 level, as well as the autocorrelation among TIP scores.